

Autocorrelation-subtracted Fourier transform holography method for large specimen imaging

Kyoung Hwan Lee, Hyeok Yun, Jae Hee Sung, Seong Ku Lee, Hwang Woon Lee, Hyung TaeK Kim, and Chang Hee Nam

Citation: *Applied Physics Letters* **106**, 061103 (2015); doi: 10.1063/1.4907641

View online: <http://dx.doi.org/10.1063/1.4907641>

View Table of Contents: <http://scitation.aip.org/content/aip/journal/apl/106/6?ver=pdfcov>

Published by the AIP Publishing

Articles you may be interested in

[Single-shot nanometer-scale holographic imaging with laser-driven x-ray laser](#)

Appl. Phys. Lett. **98**, 121105 (2011); 10.1063/1.3560466

[Multiple reference Fourier transform holography with soft x rays](#)

Appl. Phys. Lett. **89**, 163112 (2006); 10.1063/1.2364259

[Hard X-Ray Fourier Transform Holography with Zone Plates](#)

AIP Conf. Proc. **705**, 1340 (2004); 10.1063/1.1758049

[Picosecond Fourier holography using a Lloyd's mirror and an X-ray laser at 13.9 nm](#)

AIP Conf. Proc. **641**, 522 (2002); 10.1063/1.1521071

[Microscopic imaging with high energy x-rays by Fourier transform holography](#)

J. Appl. Phys. **90**, 538 (2001); 10.1063/1.1378810



Autocorrelation-subtracted Fourier transform holography method for large specimen imaging

Kyoung Hwan Lee,¹ Hyeok Yun,¹ Jae Hee Sung,^{1,2} Seong Ku Lee,^{1,2} Hwang Woon Lee,¹ Hyung TaeK Kim,^{1,2,a)} and Chang Hee Nam^{1,3,b)}

¹Center for Relativistic Laser Science, Institute for Basic Science (IBS), Gwangju 500-712, Republic of Korea

²Advanced Photonics Research Institute, Gwangju Institute of Science and Technology (GIST), Gwangju 500-712, Republic of Korea

³Department of Physics and Photon Science, Gwangju Institute of Science and Technology (GIST), Gwangju 500-712, Republic of Korea

(Received 11 November 2014; accepted 26 January 2015; published online 9 February 2015)

We developed a variation of Fourier transform holography (FTH) method to record larger objects than those tolerable in conventional FTH. This method eliminates the separation condition of FTH by removing the autocorrelation signal, thus allowing three-fold larger specimens than those previously used in FTH under the same illumination conditions. We experimentally demonstrated this FTH variation, using a table-top Ag X-ray laser at 13.9 nm, with a sample violating the separation constraint. The portion of the object image hidden behind its autocorrelation in the FTH image was recovered by subtracting an independently measured autocorrelation signal of the object. © 2015 AIP Publishing LLC. [<http://dx.doi.org/10.1063/1.4907641>]

Lensless imaging coupled with coherent X-ray source is an emerging technology used to obtain microscopic images with high spatial resolution.^{1–3} Lensless imaging can overcome the restrictions of conventional X-ray microscopes using inefficient X-ray diffractive lenses,^{4–6} because it reconstructs object images from far-field diffraction patterns by employing numerical procedures.⁷ X-ray lensless imaging methods, such as Fourier transform holography (FTH)^{8–11} and iterative phase retrieval methods,^{12–15} have common advantages of compactness, an absence of aberration, and the capability for phase object observation. In particular, FTH can immediately produce a reconstructed image without numerical ambiguities through the simple Fourier transform of a diffraction pattern.¹⁶ Thus, FTH is an attractive tool for the investigation of nanometer-scale objects that offers real-time reconstruction capability.^{17–19}

In FTH, a hologram is formed from the interference between the diffracted wave from an object and the spherical wave from a reference pinhole. For the proper reconstruction of holograms, an appropriate distance between the object and the reference, along with sufficient reference wave strength, are necessary. Even though several types of extended references have been proposed to improve the strength of weak reference waves,^{20–23} a method to overcome the problems posed by the separation condition has not been devised. Also, the FTH separation condition demands a coherent illumination area that is three times larger than the size of specimen.²¹ Thus, the limitation posed by the separation condition should be overcome in order to facilitate imaging of large specimens, especially for illumination sources with weak brightness and poor coherence.

In this letter, we propose a modified FTH method, named autocorrelation-subtracted FTH (AS-FTH), to eliminate the separation condition of FTH. AS-FTH eliminates

the separation condition by removing the autocorrelation of an object from the FTH image. This approach is advantageous when imaging large specimens with a light source of limited flux and coherence, because AS-FTH requires a much smaller coherent illumination area than the conventional FTH. In this study, the AS-FTH was performed using a table-top Ag X-ray laser, which is relatively weaker and less coherent than X-ray free electron lasers. A sample plate including a reference point violating the separation condition was prepared, and, thus, some part of the reconstructed image was veiled under the autocorrelation signal. In order to remove the autocorrelation signal, the diffraction pattern of the object without the reference pinholes was acquired separately. The hidden portion of the object image was then uncovered by subtracting the separately obtained autocorrelation signal of the object from the reconstructed image.

Conventional FTH requires a large separation between an object and a reference pinhole. The required illumination area for FTH is determined by the radius, r , of the object and the distance, d , between an object (O) and a reference pinhole (R). Figure 1(a) shows an example of a typical FTH sample (S), and the reconstructed FTH image can be described as the autocorrelation of the sample as follows:

$$S \otimes S = O \otimes O + R \otimes R + O \otimes R + R \otimes O, \quad (1)$$

where \otimes represents a correlation operator.²⁴ In the FTH image, the autocorrelation signal, $O \otimes O + R \otimes R$, with a radius of $2r$ is placed at the center and the object images ($O \otimes R$, $R \otimes O$) are placed at the distance d from the center, as shown in Fig. 1(b). In order to avoid overlapping between the object images and the autocorrelation signal, the separation condition, $d > 3r$, should be satisfied.²¹ However, if the autocorrelation signal can be removed from the reconstructed image, the separation condition can be eliminated. Since $R \otimes R$ is negligible for a tiny reference pinhole, the central autocorrelation signal can be effectively erased by

a)htkim@gist.ac.kr

b)chnam@gist.ac.kr

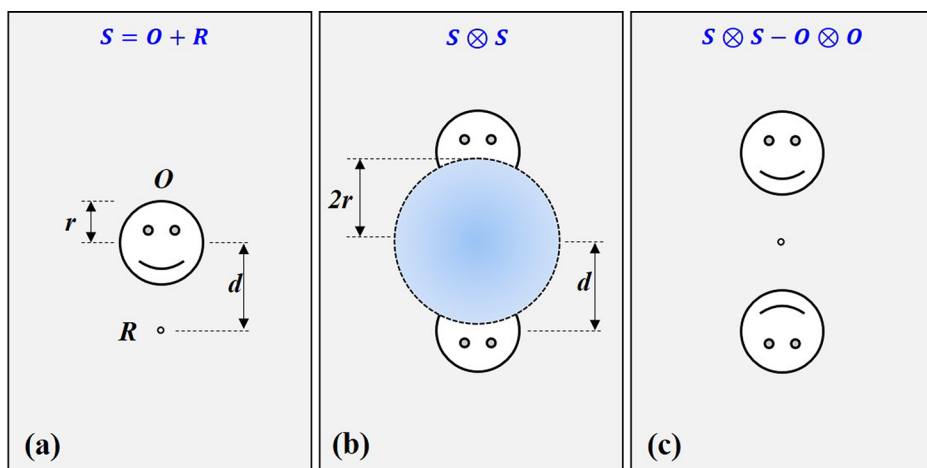


FIG. 1. Schematic diagrams showing the AS-FTH reconstruction procedure. (a) Typical FTH sample plate (S) with an object (O) and a reference (R). (b) Inverse Fourier transform of the far-field diffraction pattern of S . (c) Unveiled object signal obtained by subtracting the autocorrelation of the object.

subtracting $O \otimes O$. To this end, AS-FTH uses a separately acquired diffraction signal of O , the autocorrelation signal of which is then subtracted from the FTH image. Figure 1(c) shows the AS-FTH image of Fig. 1(a), obtained by subtracting $O \otimes O$ from Fig. 1(b). It demonstrates that the veiled portion of the object image under the autocorrelation signal in Fig. 1(b) can be recovered through AS-FTH. Even though this method requires the separate acquisition of the object diffraction, it enables a reference pinhole to be placed near the object. Therefore, AS-FTH allows obtaining a holographic image using a coherent illumination area close to the size of the object, i.e., nine-times smaller coherent photons than that required by conventional FTH.

The proposed AS-FTH technique was demonstrated using a table-top Ni-like Ag X-ray laser at 13.9-nm wavelength. Figure 2 shows the schematic layout of AS-FTH. The X-ray laser was generated from a 9-mm-long Ag medium pumped by a Ti:sapphire laser pulse with 2-J energy and 8-ps duration.²⁵ In addition, it was optimized to obtain an output power of 1.5 μJ per pulse, corresponding to 10^{11} photons. The generated X-ray laser was focused onto a sample plate by a Mo/Si multilayer mirror of 15-cm focal length and 60% reflectivity. On the sample plate, the focal spot was about

80 μm in full width half maximum. The number of coherent photons in an X-ray laser pulse was 10^9 , contained within an area of 16- μm spatial coherence length measured with the Young's double slit method.²⁶ In order to block the stray light a 200-nm Zr filter was placed in front of the sample plate. The diffraction signal from the sample plate was recorded using an X-ray CCD, having 2048×2048 pixels with a unit pixel size of 13.5 μm , located 42 mm away from the sample plate. For the sample plate, a “ h ” pattern with a size of $3 \times 5 \mu\text{m}^2$ was carved using a focused ion beam (FIB) on 300-nm-thick Au film coated on a 50-nm-thick Si_3N_4 membrane. The inset images ((i) and (ii)) in Fig. 2 are scanning electron microscope (SEM) images of the sample plates without and with 140-nm-diameter reference pinholes, respectively. In the latter sample plate, one reference pinhole satisfies the separation condition, while the other not. In the experiment, we obtained the diffraction signals of these samples separately, for the AS-FTH process.

AS-FTH was realized as follows. First, the diffraction signal of the “ h ” pattern without a reference pinhole was recorded using a single X-ray laser pulse, to define the autocorrelation signal of the object. In the reconstruction, the diffraction signal contained within the central 1024×1024 pixels was used, and the corresponding single pixel size in the reconstructed image was 42 nm. Figure 3(a) shows the diffraction signal of the “ h ” pattern, while Fig. 3(b) is its inverse Fourier transform, i.e., the autocorrelation signal of the “ h ” pattern. Then, reference pinholes were fabricated in the sample plate using FIB, and the resultant diffraction signal was acquired. Figure 3(c) shows the diffraction signal of the sample plate with reference pinholes, while Fig. 3(d) shows the reconstructed image of the sample plate. The image in Fig. 3(d) contains two independent “ h ” pattern image sets reconstructed from the two reference pinholes; one satisfies the separation condition and the other violates it. For the reference pinhole satisfying the separation condition, the images from the pinhole were clearly reconstructed. However, in the other images in Fig. 3(d), a part of the object image is hidden under the autocorrelation signal, due to the violation of the separation condition. In this case, the direct image reconstruction was not achievable.

The hidden component of the “ h ” pattern images was unveiled by subtracting the autocorrelation signal of the “ h ” pattern from the reconstructed images with the reference pinholes. For the proper subtraction of autocorrelation, the

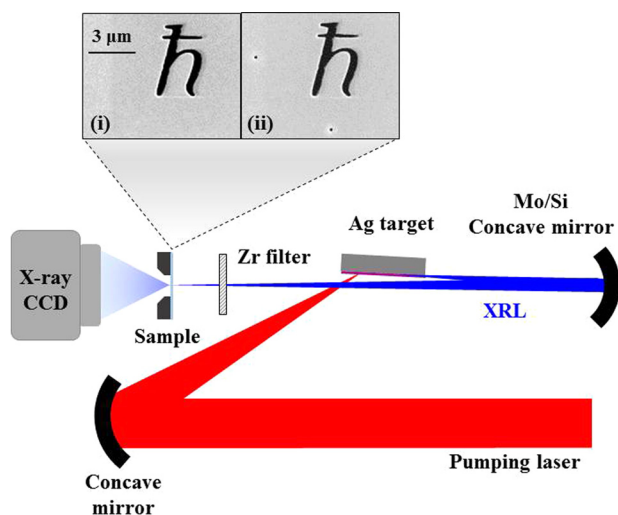


FIG. 2. Schematics of AS-FTH experimental setup using a table-top Ag X-ray laser at 13.9 nm. Inset (i) SEM image of a sample plate with a “ h ” pattern and (ii) SEM image of a same sample plate with two reference pinholes.

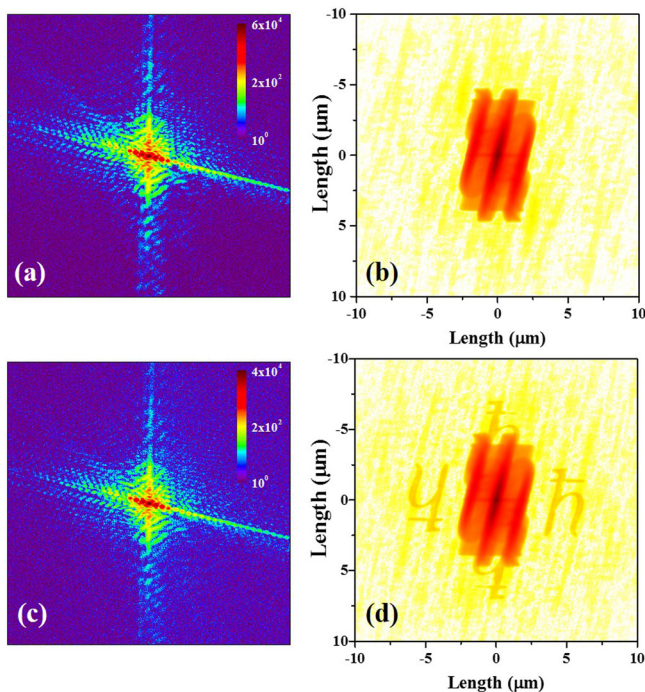


FIG. 3. (a) Diffraction signal of the “*h*” pattern without reference pinholes. (b) Inverse Fourier transform of (a) (logarithmic scale). (c) Diffraction signal of the “*h*” pattern with two reference pinholes. (d) Inverse Fourier transform of (c) (logarithmic scale).

signal level and image orientation of two autocorrelations should match, for which the diffraction signals were normalized and the orientation of samples was kept the same. Figure 4(a) shows the reconstructed AS-FTH image produced by subtracting the image in Fig. 3(b) from that of Fig. 3(d), and the shape of the revealed “*h*” pattern is clearly observable. The intensity profiles in Fig. 4(b) of the unveiled AS-FTH image (red arrow) and the normal FTH image (blue arrow) in Fig. 4(a) show almost identical except the negative signal at the left background part. The spatial resolution estimated from knife-edge method was about 140 nm and 120 nm for AS-FTH and normal FTH images, respectively.

We performed simulations of AS-FTH to analyze the image deformation appearing in the AS-FTH in Fig. 4(a). The deformation of the image can come from the change of experimental conditions between diffraction image acquisitions such as illumination change and noise. Here, we show the simulation results taken with two illumination conditions—one with uniform intensity and the others with linear intensity distribution, as the noise effect was less significant in the simulations. With 15% intensity variation along the “*h*” pattern, as shown in the inset of Fig. 4(c), the calculated AS-FTH image in Fig. 4(c) shows a reconstructed image comparable to that of the experimental result. Figure 4(d) shows the intensity profiles of AS-FTH measured along the red arrow in Fig. 4(c) for the cases of uniform intensity (blue dots), and linear intensity variation of 5% (black triangles) and 15% (red squares). In the case of the 15% intensity variation, the negative background is noticeable at the left edge, while it was not significant in the case of 5% intensity variation. Thus, the simulation result shows that the deformation of experimental AS-FTH image originated mainly from the spatial intensity variation of

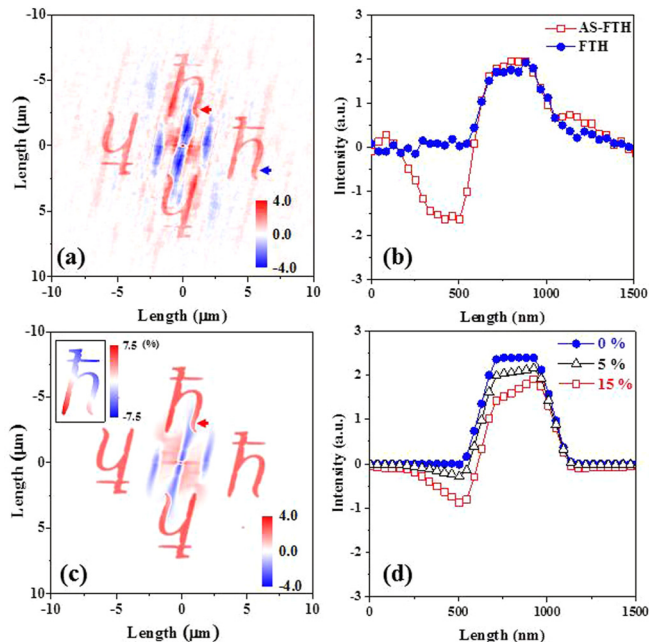


FIG. 4. (a) Autocorrelation-subtracted FTH image, i.e., the image in Fig. 3(d)—that in Fig. 3(b). (b) Intensity profiles of the reconstructed “*h*” pattern image measured along the red (red squares) and the blue (blue dots) arrows in Fig. 4(a). (c) Simulated AS-FTH image obtained with an intensity distribution of 15% linear variation. The inset shows the intensity variation between two diffraction image acquisitions. (d) Intensity profiles along the red arrow in Fig. 4(c) for the cases of uniform intensity (blue dots), and linear intensity variation of 5% (black triangles) and 15% (red squares).

the x-ray laser beam, which can be improved by minimizing the intensity variation of a light source.

In order to obtain proper reconstruction of AS-FTH in practical situations, the reconstructed object signal, i.e., cross-correlation signal, should be stronger than the background signal from the remnant after the subtraction of the autocorrelation signal. One solution is to suppress the background signal by minimizing the illumination change during two image acquisitions. For this purpose, an in-line mask can be introduced to block and open the reference pinhole so that two image acquisitions can be performed in a short time interval. The AS-FTH coupled with the in-line blocker can be a practical solution for real applications. Another possible approach is to increase the intensity of cross-correlation signal using a strong reference wave. This can be achieved by introducing an extended reference, used in the “holography with extended reference by autocorrelation linear differential operation” (HERALDO).^{21,27} In applying HERALDO to AS-FTH, the contribution of the autocorrelation signal by an extended reference should be negligible by adopting a thin line reference so that the autocorrelation signal could be properly subtracted. Therefore, the limitation of AS-FTH can be improved using in-line mask and producing strong reference wave.

In summary, we have obtained the holographic image of a sample violating the separation condition of FTH by applying the AS-FTH method. This technique allows the recovery of the reconstructed image buried under the autocorrelation signal. By eliminating the separation condition using AS-FTH, the reference pinhole for FTH can be located close to the sample boundary, reducing significantly the required area of coherent illumination in FTH. In another sense, for a

given illumination condition, the size of a sample can be three times larger than that of the nominal FTH. Equivalently, AS-FTH makes it possible to obtain holographic images with a weak illumination source by reducing the illumination area using stronger focus close to the size of samples. Consequently, the AS-FTH method will be a powerful imaging technique for investigating large specimens using a tabletop coherent X-ray source.

This work was supported by IBS (Institute for Basic Science) under IBS-R012-D1.

- ¹P. W. Wachulak, M. C. Marconi, R. A. Bartels, C. S. Menoni, and J. J. Rocca, *J. Opt. Soc. Am. B* **25**, 1811 (2008).
- ²M. D. Seaberg, D. E. Adams, E. L. Townsend, D. A. Raymondson, W. F. Schlotter, Y. Liu, C. S. Menoni, L. Rong, C.-C. Chen, J. Miao, H. C. Kapteyn, and M. M. Murnane, *Opt. Express* **19**, 22470 (2011).
- ³C. G. Schroer, P. Boye, J. M. Feldkamp, J. Patommel, A. Schropp, A. Schwab, S. Stephan, M. Burghammer, S. Schöder, and C. Riekel, *Phys. Rev. Lett.* **101**, 090801 (2008).
- ⁴W. Chao, B. D. Harteneck, J. A. Liddle, E. H. Anderson, and D. T. Attwood, *Nature* **435**, 1210 (2005).
- ⁵K. H. Lee, S. B. Park, H. Singhal, and C. H. Nam, *Opt. Lett.* **38**, 1253 (2013).
- ⁶C. A. Brewer, F. Brizuela, P. Wachulak, D. H. Martz, W. Chao, E. H. Anderson, D. T. Attwood, A. V. Vinogradov, I. A. Artyukov, A. G. Ponomareko, V. V. Kondratenko, M. C. Marconi, J. J. Rocca, and C. S. Menoni, *Opt. Lett.* **33**, 518 (2008).
- ⁷J. R. Fienup, *Appl. Opt.* **21**, 2758 (1982).
- ⁸I. McNulty, J. Kirz, C. Jacobsen, E. H. Anderson, M. R. Howells, and D. P. Kern, *Science* **256**, 1009 (1992).
- ⁹S. Eisebitt, J. Lüning, W. F. Schlotter, M. Lörger, O. Hellwig, W. Eberhardt, and J. Stöhr, *Nature* **432**, 885 (2004).
- ¹⁰R. L. Sandberg, D. A. Raymondson, C. La-o vorakiat, A. Paul, K. S. Raines, J. Miao, M. M. Murnane, H. C. Kapteyn, and W. F. Schlotter, *Opt. Lett.* **34**, 1618 (2009).
- ¹¹W. F. Schlotter, R. Rick, K. Chen, A. Scherz, J. Stöhr, J. Lüning, S. Eisebitt, C. Günther, W. Eberhardt, O. Hellwig, and I. McNulty, *Appl. Phys. Lett.* **89**, 163112 (2006).
- ¹²A. Barty, S. Boutet, M. J. Bogan, S. Hau-Riege, S. Marchesini, K. Sokolowski-Tinten, N. Stojanovic, R. Tobey, H. Ehrke, A. Cavalleri, S. Düsterer, M. Frank, S. Bajt, B. W. Woods, M. M. Seibert, J. Hajdu, R. Treusch, and H. N. Chapman, *Nat. Photonics* **2**, 415 (2008).
- ¹³H. N. Chapman, A. Barty, M. J. Bogan, S. Boutet, M. Frank, S. P. Hau-Riege, S. Marchesini, B. W. Woods, S. Bajt, W. H. Benner, R. A. London, E. Plönjes, M. Kuhlmann, R. Treusch, S. Düsterer, T. Tschentscher, J. R. Schneider, E. Spiller, T. Möller, C. Bostedt, M. Hoener, D. A. Shapiro, K. O. Hodgson, D. van der Spoel, F. Burmeister, M. Bergh, C. Caleman, G. Hult, M. M. Seibert, F. R. N. C. Maia, R. W. Lee, A. Szöke, N. Timneanu, and J. Hajdu, *Nat. Phys.* **2**, 839 (2006).
- ¹⁴J. Miao, P. Charalambous, J. Kirz, and D. Sayre, *Nature* **400**, 342 (1999).
- ¹⁵C. Song, H. Jiang, A. Mancuso, B. Amirbekian, L. Peng, R. Sun, S. S. Shah, Z. H. Zhou, T. Ishikawa, and J. Miao, *Phys. Rev. Lett.* **101**, 158101 (2008).
- ¹⁶J. Goodman, *Introduction to Fourier Optics*, 3rd ed. (Roberts and Company Publishers, Englewood, CO, 2004).
- ¹⁷H. T. Kim, I. J. Kim, C. M. Kim, T. M. Jeong, T. J. Yu, S. K. Lee, J. H. Sung, J. W. Yoon, H. Yun, S. C. Jeon, I. W. Choi, and J. Lee, *Appl. Phys. Lett.* **98**, 121105 (2011).
- ¹⁸W. F. Schlotter, J. Lüning, R. Rick, K. Chen, A. Scherz, S. Eisebitt, C. M. Günther, W. Eberhardt, O. Hellwig, and J. Stöhr, *Opt. Lett.* **32**, 3110 (2007).
- ¹⁹T. Wang, D. Zhu, B. Wu, C. Graves, S. Schaffert, T. Rander, L. Müller, B. Vodungbo, C. Baumier, D. P. Bernstein, B. Bräuer, V. Cros, S. de Jong, R. Delaunay, A. Fognini, R. Kukreja, S. Lee, V. López-Flores, J. Mohanty, B. Pfau, H. Popescu, M. Sacchi, A. B. Sardinha, F. Sirotti, P. Zeitoun, M. Messerschmidt, J. J. Turner, W. F. Schlotter, O. Hellwig, R. Mattana, N. Jaouen, F. Fortuna, Y. Acremann, C. Gutt, H. A. Dürr, E. Beaurepaire, C. Boeglin, S. Eisebitt, G. Grübel, J. Lüning, J. Stöhr, and A. O. Scherz, *Phys. Rev. Lett.* **108**, 267403 (2012).
- ²⁰S. Marchesini, S. Boutet, A. E. Sakdinawat, M. J. Bogan, S. Bajt, A. Barty, H. N. Chapman, M. Frank, S. P. Hau-Riege, A. Szöke, C. Cui, D. A. Shapiro, M. R. Howells, J. C. H. Spence, J. W. Shaevitz, J. Y. Lee, J. Hajdu, and M. M. Seibert, *Nat. Photonics* **2**, 560 (2008).
- ²¹M. Guizar-Sicairos and J. R. Fienup, *Opt. Express* **15**, 17592 (2007).
- ²²D. Zhu, M. Guizar-Sicairos, B. Wu, A. Scherz, Y. Acremann, T. Tyliczszak, P. Fischer, N. Friedenberger, K. Ollefs, M. Farle, J. R. Fienup, and J. Stöhr, *Phys. Rev. Lett.* **105**, 043901 (2010).
- ²³H. He, U. Weierstall, J. C. H. Spence, M. Howells, H. A. Padmore, S. Marchesini, and H. N. Chapman, *Appl. Phys. Lett.* **85**, 2454 (2004).
- ²⁴R. L. Easton, Jr., *Fourier Methods in Imaging* (John Wiley & Sons, 2010).
- ²⁵H. T. Kim, I. W. Choi, N. Hafz, J. H. Sung, T. J. Yu, K.-H. Hong, T. M. Jeong, Y.-C. Noh, D.-K. Ko, K. A. Janulewicz, J. Tümmler, P. V. Nickles, W. Sandner, and J. Lee, *Phys. Rev. A* **77**, 023807 (2008).
- ²⁶H. T. Kim, K. A. Janulewicz, C. M. Kim, I. W. Choi, J. H. Sung, T. J. Yu, S. K. Lee, T. M. Jeong, D.-K. Ko, P. V. Nickles, J. Tümmler, and J. Lee, *X-Ray Lasers 2008*, Springer Proceedings in Physics, Vol. 130, edited by C. Lewis and D. Riley (Springer, Netherlands, 2009), pp. 143–152.
- ²⁷D. Gauthier, M. Guizar-Sicairos, X. Ge, W. Boutou, B. Carré, J. R. Fienup, and H. Merdji, *Phys. Rev. Lett.* **105**, 093901 (2010).